Contents lists available at ScienceDirect

Corrosion Science

journal homepage: www.elsevier.com/locate/corsci

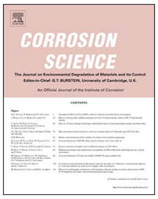

Corrosion fatigue and microstructural characterisation of Type 316 austenitic stainless steels tested in PWR primary water

K. Mukahiwa[a], F. Scenini[a,*], M.G. Burke[a], N. Platts[b], D.R. Tice[b], J.W. Stairmand[b]

[a] *Materials Performance Centre, The University of Manchester, Sackville Street Campus, Manchester, M13 9PL, UK*
[b] *AMEC Foster Wheeler, Walton House, Birchwood, Warrington WA3 6GA, UK*

ARTICLE INFO

Keywords:
A. Stainless steel
C. Corrosion fatigue
C. Hydrogen embrittlement

ABSTRACT

Fatigue crack growth experiments have been performed on high and low sulphur Type 316 austenitic stainless steel specimens in simulated Pressurised Water Reactor primary coolant environments and evaluated via microstructural characterisation techniques to further the understanding of the mechanistic behaviour. At relatively high loading frequencies, the enhanced crack growth for both specimens appeared to be crystallographic and associated with slip localization. However, when the loading frequency was decreased, the crack growth rates for the low S specimen increased, whereas the high S specimen exhibited retarded crack growth and the crack path was no longer crystallographic.

1. Introduction

In recent years, extensive experiments on pre-cracked austenitic stainless steel compact tension, (C(T)), specimens in simulated pressurised water reactor (PWR) primary coolant environments have shown that their fatigue crack growth rates (CGRs) can be enhanced substantially relative to crack growth rates in air [1–19]. In most instances, the degree of environmental enhancement increases as the applied loading frequency is reduced. Conversely, for some heats and under certain conditions of loading rate, temperature and flow rate, the fatigue crack growth can be reduced to rates marginally higher or even lower than the rates in an air environment [1,3,4,7,8,14–17]. This reduction is often termed “retardation”. The most significant factor influencing retardation appears to be a high sulphur content of the steel [1,3,4,7,8,14–17].

Enhanced fatigue crack growth of austenitic stainless steels and Nickel based alloys in PWR primary coolant environments is believed to be associated with hydrogen effects [1,2,9,13,15,18,20], although there is no direct evidence for this mechanism. The effects of hydrogen on metals and alloys can be broadly grouped into three main theories: 1) hydrogen-enhanced decohesion (HEDE) [21–24]. 2) hydrogen-enhanced localised plasticity (HELP) [25,26]; and 3) hydrogen-enhanced strain-induced vacancy formation (HESIV) [27,28]. The suggestion that hydrogen absorbed at the crack-tip of an advancing fatigue crack is responsible for enhanced fatigue crack growth is based on the similarity of microstructural features noted after testing with those expected for hydrogen-charged materials. In fact, stainless steels tested in high temperature water show evidence of formation of micro-cleavage cracks [18,29], planar fracture surfaces which are similar to those observed on hydrogen-charged specimens that are fatigue-tested in air [1,30] and apparent pile-up of planar dislocations at the crack-tip of specimens fatigue-tested in high temperature water [10–12]. Furthermore, enhancement of fatigue crack growth of hydrogen charged austenitic stainless steel specimens in air increases with decreasing loading frequency [31] similar to the fatigue crack growth of stainless steels in high temperature water. However, below a critical frequency, the fatigue crack growth of stainless steel in high temperature water can be retarded significantly to a value that can be lower than the CGR in air. The propensity for retardation increases with decreasing frequency and has been found to strongly depend on the sulphur content of the steel; specifically, high sulphur specimens retard at higher strain rates than low sulphur specimens [1,3,4,7,8,14–17].

Amongst the proposed mechanisms to explain the corrosion fatigue retardation there are three that are the most likely and all account for the beneficial effect associated with the presence of S^{2-} anions deriving from the dissolution of MnS inclusions and the stress ratio. Evidence for this is provided by tests by Platts et al., which showed that retardation can be induced in a low sulphur steel when sulphide is injected into the crack enclave [3]. The main mechanisms considered are: 1) oxide-induced crack closure (OICC) at low load ratio [1,14], 2) corrosive crack-tip blunting (CCB) [17], and 3) injected vacancy-enhanced creep (IVEC) [1,15]. OICC occurs when the fracture surfaces within a crack come in contact during the unloading phase of fatigue cycling due to the presence of oxide or oxide debris between the fracture surfaces. This results

---

* Corresponding author.
E-mail address: fabio.scenini@manchester.ac.uk (F. Scenini).

https://doi.org/10.1016/j.corsci.2017.10.022
Received 24 December 2016; Received in revised form 19 September 2017; Accepted 25 October 2017

Please cite this article as: Mukahiwa, K., Corrosion Science (2017), http://dx.doi.org/10.1016/j.corsci.2017.10.022

in a reduction of the effective stress intensity factor range (ΔK) and consequently crack growth per cycle (da/dN) according to the Paris Law [1,14,32,33]. CCB is due to the active corrosion in the crack-tip region, which alters the geometry to reduce the sharpness of the crack [17,34,35], lowers the stress/strain field around the crack, reduces the ΔK, and ultimately the crack growth rate decreases. A variation to this mechanism is IVEC in which the injected vacancies generated from the oxidation process promote low temperature creep around the crack-tip and redistribution of the stress [1,15].

Despite the extensive effort by many laboratories, the mechanisms for crack enhancement and retardation of austenitic stainless steels in high temperature water under specific circumstances are still unclear. Therefore, the aim of this work is to provide insight into the mechanisms of fatigue crack growth behaviour via the microstructural characterisation of Type 316 austenitic stainless steels tested in high temperature water under cyclic loading. This study involves the characterisation of two heats of 316 austenitic stainless steel with different sulphur contents that were fatigue-tested under identical nominal load and water chemistry in a simulated PWR primary coolant environment. Fractographic characterization was performed to investigate the crack topography, to examine the oxide formed on the fracture surface and to identify any possible location where crack closure occurred. The crack paths for the unbroken samples were investigated using advanced electron microscopy and diffraction analyses to identify strain localization at the advancing cracks.

2. Experimental details

2.1. Materials

The fatigue crack growth tests were performed on two solution-annealed Type 316 austenitic stainless steels that had a similar composition but varied in S content. One sample had a low sulphur content (0.002 wt%) and was designated as “LS”, whilst the other contained 0.012 wt% S and was designated as “HS”. The other main compositional difference was that the HS specimen was L-grade (C = 0.02%) whilst the LS specimen was high carbon (C = 0.044%) type 316 austenitic stainless steel. The compositions of the two steels are listed in Table 1. These two heats were chosen to investigate primarily the effect of the difference in sulphur on the fatigue crack growth behaviour. In fact, previous work has shown that the influence of carbon content on environmentally enhanced fatigue crack growth in PWR environments is much less than that of sulphur for both Types 304 and 316 austenitic stainless steels [3,17].

2.2. Fatigue crack growth testing

Two fatigue crack growth tests were performed at temperatures between 250 and 300 °C in high purity hydrogenated water containing 2 ppm of Li (added as LiOH) and H_2 (35–45) cc/kg H_2O. The experiments were conducted in a refreshed flow loop which was similar to the one previously used by some of the present authors [3,4,8,36,37]. The experiments were performed on air fatigue pre-cracked 25 mm C(T) specimens without side grooves. The specimens were loaded in a chain of up to three samples and were insulated from the loading chain via oxidised Zircaloy bushes. The crack growth rate for each specimen was continuously monitored using a reverse direct current potential drop (DCPD) crack growth monitoring system. Throughout the test, the specimens were cyclically loaded using an asymmetric saw tooth waveform that was approximately 85% rise-time and 15% fall-time. Prior to test start-up, the autoclave containing the test samples was purged with nitrogen at room temperature and the feed tank test solution deaerated with nitrogen to a dissolved oxygen content of less than 5 ppb with dissolved oxygen content measured continuously at the autoclave outlet using a Hach-Lange Luminescent Dissolved Oxygen meter. A hydrogen overpressure on the feed tank was then established and the system brought up to high temperature, high pressure conditions. A total of two tests were carried out to produce samples for fractographic examinations (Test 1) and to examine the crack path in cross section (Test 2). More details of these two tests are reported in the subsections below.

Table 1
Composition (wt%) of Type 316 Stainless Steels.

Specimen	C	Si	Mn	Cr	Ni	S	P	N	Mo
HS	0.02	0.59	1.71	16.95	11.29	0.012	0.005	0.06	2.2
LS	0.044	0.39	1.71	16.8	10.22	0.002	0.03	0.072	2.1

Test 1 was performed on two 25 mm C(T) specimens, one LS and one HS. The initial pre-crack length of the HS specimen was 19.185 mm whilst that of the LS specimen was 18.629 mm. The initial $K_{\max}$ values for the HS and LS specimens were 24.7 MPa√m and 24.0 MPa√m, respectively. The applied stress ratio ($R = K_{min}/K_{max}$) was maintained at 0.7 throughout the environmental test. The rise-time and/or temperature were changed 12 times and the parameters for each of the 12 stages are summarised in Table 2. After the 12 stages of environmental growth, the C(T) specimens were broken open by fatigue in air at an R ratio of 0.1 to reveal the fracture surfaces.

Test 2 was performed to generate specimens for crack cross-section and crack-tip analysis to identify the difference in the crack-tip deformation during enhancement and retardation. The environmental conditions in the test, the DCPD crack growth monitoring system and the loading waveform were the same as in the first three stages of Test 1. The C(T) specimen thickness for the HS specimen was ~24.5 mm, whilst the thickness of the LS specimen was ~23.9 mm. The initial pre-crack length of the HS specimen was 17.70 mm whilst that of the LS specimen was 18.60 mm. The initial $K_{\max}$ values for the HS and LS specimens were 24.6 MPa√m and 26.4 MPa√m respectively. The R ratio was maintained at 0.7 throughout the environmental test.

2.3. Microstructural and fractographic characterisation

The baseline microstructural characterisations of the HS and LS specimens were performed on offcuts of the material originally used to manufacture the C(T) samples and in the same plane as the cracking plane, and the plane parallel to the crack side flanks. The coupons were then ground to 4000 grit on silicon carbide paper before being polished with 3 and 1 μm polycrystalline diamond suspension solution respectively. The final polishing step was with a 0.04 μm Metprep Colloidal Silica solution (OPS). To make the cross-section of the crack path of specimens from test 2 suitable for electron microscopy characterisation, unbroken tested HS and LS CT specimens were cut into 1 mm thick slices that were parallel to the crack growth direction using an electro discharge machine. Thereafter the slices were polished using the polishing procedure outlined.

The microstructure of the various specimens was characterised using a Keyence Laser Scanning Confocal Microscope, FEI Quanta 650 Field Emission Gun Environmental Scanning Electron Microscope (FEG-ESEM), FEI Megellan FEG-SEM and a Zeiss Ultra 55 FEG-SEM. All FEG-SEMs were equipped with Oxford HKL high resolution EBSD detectors and energy dispersive X-ray (EDX) spectrum imaging and analysis systems. Site-specific cross-sections of the fatigue-tested specimens were prepared using the focused ion beam (FIB) technique. An FEI Quanta 3D FIB was used for the preparation of cross-sections from selected locations on the fractured samples.

High spatial resolution EBSD analysis of the corrosion fatigue crack-tip regions in both LS and HS specimens was performed using the FEI Magellan FEG-SEM with AztecHKL software. The accelerating voltage was 15 kV. For the EBSD analysis, the sample was mounted on a specimen holder with a 10° pre-tilt, which was then tilted a further 60° towards the EBSD detector. The high resolution EBSD data sets were